Available online at www.sciencedirect.com
ScienceDirect
Journal of the European Ceramic Society 30 (2010) 1373–1380
www.elsevier.com/locate/jeurceramsoc

Pressureless sintering of carbon nanotube–Al_2O_3 composites

Shi C. Zhang [a,*], William G. Fahrenholtz [a], Greg E. Hilmas [a], Edward J. Yadlowsky [b]

[a] *Department of Materials Science and Engineering, Missouri University of Science and Technology, Rolla, MO 65401, USA*
[b] *HY-Tech Research Corporation, Radford, VA 24141, USA*

Received 8 September 2009; received in revised form 11 November 2009; accepted 1 December 2009
Available online 31 December 2009

Abstract

Alumina ceramics reinforced with 1, 3, or 5 vol.% multi-walled carbon nanotubes (CNTs) were densified by pressureless sintering. Commercial CNTs were purified by acid treatment and then dispersed in water at pH 12. The dispersed CNTs were mixed with Al_2O_3 powder, which was also dispersed in water at pH 12. The mixture was freeze dried to prevent segregation by differential sedimentation during solvent evaporation. Cylindrical pellets were formed by uniaxial pressing and then densified by heating in flowing argon. The resulting pellets had relative densities as high as ~99% after sintering at 1500 °C for 2 h. Higher temperatures or longer times resulted in lower densities and weight loss due to degradation of the CNTs by reaction with the Al_2O_3. A CNT/Al_2O_3 composite containing 1 vol.% CNT had a higher flexure strength (~540 MPa) than pure Al_2O_3 densified under similar conditions (~400 MPa). Improved fracture toughness of CNT–Al_2O_3 composites was attributed to CNT pullout. This study has shown, for the first time, that CNT/Al_2O_3 composites can be densified by pressureless sintering without damage to the CNTs.

Keywords: Carbon nanotubes; Al_2O_3; Composites; Mechanical properties

1. Introduction

Carbon nanotubes (CNTs), first reported by Iijima,[1] have excellent mechanical properties, including an ultra-high elastic modulus of ~1 TPa and a high tensile strength of >10 GPa.[2,3] In addition, CNTs have good chemical stability. Therefore, CNTs are attractive candidates for reinforcement of various materials. Many studies have focused on using CNTs to enhance the mechanical properties of metal, ceramic, or polymer based composites.[4] In some cases, CNTs can even replace carbon fibers.[5,6] In particular, attention has been paid to enhancing mechanical properties of polymers[2,7–9,11–15] and metals.[2,6,10,16] Relatively few reports discuss CNT-reinforced ceramics, with the majority of those reports discussing alumina (Al_2O_3).[2,10,17–27,28]

Several key problems exist in the fabrication of CNT–Al_2O_3 composites.[20,23] The first problem is dispersion of CNTs in the Al_2O_3 matrix. Usually, CNTs are synthesized by catalytic chemical vapor deposition (CCVD),[4,25,29] which results in a very high aspect ratio of 30–10,000[4,25] and strong Van der Waals forces between the tubes. As a result, both single- and multi-walled CNTs form twisted aggregate structures[30] that are difficult to disperse. To obtain a CNT–Al_2O_3 composite with a homogeneous CNT distribution, several approaches have been investigated. One is the *in situ* synthesis of CNTs on ceramic powders, which has been reported by several research groups.[4,10,19,28] In this process, ceramic powders are mixed with fine transition metal particles, such as Fe, Co or Ni, which serve as the catalyst for CNT growth. Gases that serve as carbon sources, such as CH_4–H_2[4,10] or C_2H_2–Ar–H_2,[18,28] are then flowed through the powders. The gases decompose and CNTs grow from the transition metal particles, which results in the formation of CNT–ceramic composite powders. However, the CNTs are not homogeneously distributed in the as-synthesized state. Consequently, the synthesized composite powders require further mixing by ball or attrition milling.[10] *In situ* synthesis also leads to a second problem, which is deposition of residual amorphous carbon during growth.[10,31] The presence of residual carbon adversely affects the strength of the CNT–Al_2O_3 composites.

Another approach to disperse CNTs in ceramic powders is to prepare slurries of Al_2O_3 and CNTs using techniques such as ultrasonic agitation or ball milling with surfactant

* Corresponding author at: Department of Materials Science and Engineering, Missouri University of Science and Technology, 222 McNutt Hall, 1870 Miner Circle, Rolla, MO 65401, USA. Tel.: +1 573 341 4092; fax: +1 573 341 6934.
E-mail address: scz@mst.edu (S.C. Zhang).

0955-2219/$ – see front matter © 2009 Elsevier Ltd. All rights reserved.
doi:10.1016/j.jeurceramsoc.2009.12.005

additions.[8,21,30] However, the density of CNTs ranges[23] from 1 to 2 g/cm^3 compared to ~4 g/cm^3 for Al_2O_3, which can lead to segregation during drying due to the different sedimentation rates of the two materials. In addition, CNTs have sp^2 hybrid covalent bonding[6] whereas Al_2O_3 has a significant ionic bonding character. The difference in bond character affects the surface charges that develop when the two materials are dispersed in polar solvents as well as their response to surfactant additions. The differences in density and bonding tend to promote segregation of CNTs from Al_2O_3 particles in suspensions and during drying. Consequently, CNT aggregates have been observed in CNT–Al_2O_3 composites produced by hot-pressing powders in which CNTs were dispersed by ultrasonic agitation and ball milling.[21]

Previous studies[32,33] have shown that densification of ceramics can be inhibited by the presence of inclusions, such as CNTs, in the matrix. This is why all CNT–Al_2O_3 composites reported to date have been fabricated by hot-pressing[4,19–27] or spark plasma sintering (SPS).[8,18,30] However, hot-pressing and SPS are limited to the formation of simple geometries and moderate sizes. Development of pressureless sintering processes is needed to enable the commercially viable fabrication of complex geometries to near-net shape using standard ceramic powder processing methods. As with other composite systems, it should be possible to develop a pressureless sintering process for CNT–Al_2O_3 composites. The CNTs may have a beneficial effect on the resulting composite by reducing the grain size of the matrix through physical pinning of grain boundaries. Generally, reducing the grain size increases the strength of the resulting composite compared to the nominally pure matrix material.

The objectives of the present study are to minimize the segregation of CNTs from Al_2O_3 during powder processing and to densify CNT–Al_2O_3 compacts by pressureless sintering.

2. Experimental procedure

2.1. Raw materials

Commercial multi-walled carbon nanotubes (MWCNTs) (95+%, OD 30–50 nm, length 0.5–2 μm, NanoAmor, Houston, TX) and alumina powder (RC-HP-DBM, Baikowski-Malakoff, Malakoff, TX) were the raw materials used for this study. The Al_2O_3 powder had an average particle size of 0.5 μm and a surface area of 3.75 m^2/g.

2.2. Mixing approaches

The as-received commercial MWCNTs were suspended in a mixture of 300 ml concentrated sulfuric acid (H_2SO_4) and 100 ml concentrated nitric acid (HNO_3). The mixture was sonicated for 3 h and then stirred for 24 h. After stirring, the MWCNT suspension was filtered using a 0.1 μm nylon filter membrane (Nalgene Disposable Filterware, Nalgene Co., Rochester, NY), followed by washing with distilled water until the pH of the filtrate was near 7. The MWCNTs were dried at 100 °C overnight.

The Al_2O_3 powder was sonicated and stirred in water with its pH adjusted to 12 using NH_4OH. The resulting slurry was milled using Al_2O_3 media for 24 h.

The purified and dried MWCNTs were weighed to produce composites containing 1, 3 or 5 vol.% CNTs, based on reported densities of 2.1 g/cm^3 for MWCNTs[34] and 3.96 g/cm^3 for alumina. The MWCNTs were dispersed in water with its pH adjusted to 12 using NH_4OH.[35] The MWCNTs were dispersed by ultrasonic agitation and stirring for 30 min. Additional NH_4OH was added to keep the pH of the water at ~12.

The Al_2O_3 slurry was added to the dispersed MWCNT suspension under ultrasonic agitation and stirring. The mixed slurry was then ball milled for 30 min. To minimize MWCNT segregation, the mixed slurry was immediately dried in a freeze dryer (Genesis 25 SQ Freeze Dryer, VirTis Co., Gardiner, NY) at −20 °C and ~13 Pa (100 mTorr) for 48 h.

2.3. Densification

For the densification studies, 19 mm diameter pellets were formed by uniaxial dry pressing at 19 MPa (2.7 ksi) followed by cold isostatic pressing at 310 MPa (45 ksi). For the mechanical properties study, rectangular specimens with dimensions of 25 mm × 50 mm × 6 mm were formed using the pressing pressures.

All of the densification studies were conducted using a graphite crucible in a resistance heated graphite element furnace (3060-FP20, Thermal Technology Inc., Santa Rosa, CA). Pressed pellets were heated at 10 °C/min to the sintering temperature (1500 or 1600 °C) for densification. The furnace atmosphere was flowing argon (~10^5 Pa). The pellets were held at the specified sintering temperatures for 1–2 h.

Bulk densities of sintered specimens were measured using Archimedes' method with water as the immersing medium. Relative densities were calculated by dividing the measured bulk density by the appropriate theoretical density, which was calculated using a volumetric rule of mixtures based on densities of 3.98 g/cm^3 for Al_2O_3 and 2.1 g/cm^3 for the MWCNTs.

2.4. Characterization

Flexure strength was measured in four point bending according to ASTM C1161-02a for type A bars (1.5 mm × 2.0 mm × 25 mm) using a screw-driven test frame (Model 5881, Instron Corp., Norwood, MA). The reported values of flexure strength were averaged based on eight specimens for each composition. The elastic moduli were measured according to ASTM Standard C1259-01 for impulse excitation of cylindrical discs (Grindosonic, J.W. Lemmens, St. Louis, MO). Vickers' hardness was determined from a minimum of 10 indents formed using a load of 200 g and a dwell time of 15 s (Duramin 5, Struers, Westlake, OH). Fracture toughness was determined by the indentation strength in bending method.[36] Radial–median cracks were produced in the bend bars by indentation using a load of 10 kg and a dwell time of 10 s. Retained strength was measured in four point bending. The reported values of fracture toughness were averaged based on eight specimens.

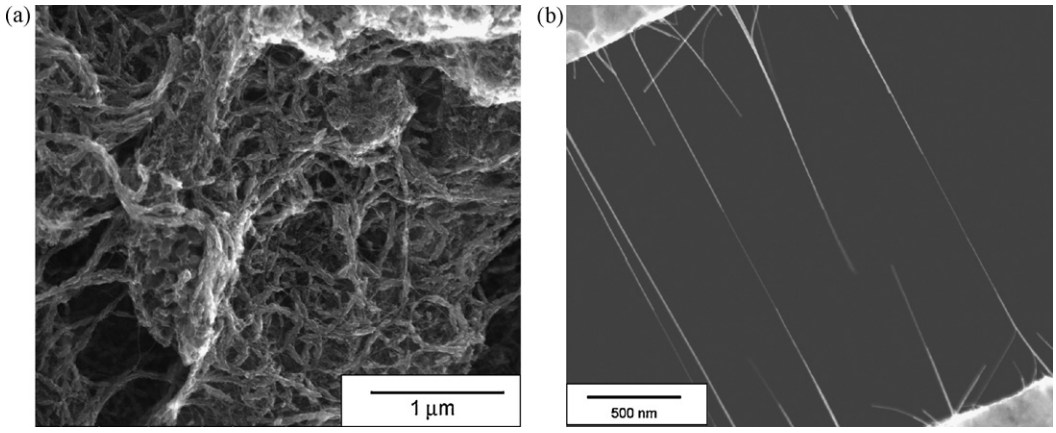

Fig. 1. Comparison of the microstructures of MWCNTs (a) before and (b) after acid. purification.

The fracture surfaces were observed using scanning electron microscopy (SEM S-4700 Hitachi, Japan). The electrical resistivity of Al_2O_3–CNT composites was calculated from leaking currents measured under various DC voltages using an electrometer (6517A Electrometer/High Resistance Meter, Kethley, US). Both sides of sintered pellets were ground flat and parallel followed by coating with instant drying silver paste to produce electrodes.

3. Results and discussion

3.1. Purification and dispersion of CNTs

The commercial MWCNTs used in the present study were synthesized by the CCVD method and their purity was reported to be more than 95 wt.%.[34] The impurities in the MWCNTs typically include transition metal catalyst particles, amorphous carbon, and nanocrystalline graphite.[31,35] Because these impurities can degrade the strength of sintered CNT–Al_2O_3 composites, the MWCNTs were purified prior to use. In addition, the CNTs have covalent bonds and are not readily dispersible in polar liquids such as water. So, the surfaces were also modified. Oxidation in a liquid medium is a common method used to purify and modify CNTs since it can remove both metal catalysts and amorphous carbon.[23] In the present study, five grams of the as-received commercial MWCNTs were purified and oxidized in a mixed solution of concentrated sulfuric acid (H_2SO_4) and concentrated nitric acid (HNO_3).

Fig. 1 compares the micromophology of as-received and purified MWCNTs. The as-received MWCNTs were agglomerated, forming an intertwined structure. In contrast, the purified MWCNTs were visibly separated and single CNTs could be observed. To assess the impact of the purification on the properties of the CNTs, both as-received and purified MWCNTs were dispersed in water at pH 12 and then allowed to settle for one week (Fig. 2). The purified CNTs were much more stable in water. Even though the suspension was left undisturbed for one week, the purified MWCNTs remained suspended. In contrast, the as-received CNTs settled out of suspension in less than 1 h. Poyato et al. have reported similar results[34] and indicated that purification of CNTs using sulfuric and nitric acids had two effects: first, the treatment removed impurities, including metal catalyst particles and amorphous carbon. The amorphous carbon was removed in preference to the CNTs because amorphous carbon has a higher chemical activity than the crystalline carbon nanotubes. Second, the MWCNT surfaces were oxidized. The presence of oxygenated functional groups, such as hydroxyl or carboxyl groups, has been confirmed in other studies using Raman spectroscopy.[23,34] The hydroxyl or carboxyl groups allow the purified CNTs to be readily dispersed in water.

3.2. Mixing and drying of MWCNTs and Al_2O_3

Preparation of well mixed CNT and Al_2O_3 powders is a key step for preparing high quality CNT–Al_2O_3 composites. The purified MWCNTs can be dispersed in water at pH 12, which is above the isoelectric point for Al_2O_3 (IEP ~7–9).

Fig. 2. Settling tests of as-received MWCNTs (left) and purified MWCNTs (right) in water at pH 12.

Table 1
Summary of thermodynamic analysis of possible reactions in the Al_2O_3–C system.

Reactions		$\Delta G^{\circ}_{r\times n}$ (kJ)	Favorable (°C)
$2Al_2O_3 + 9C \rightarrow Al_4C_3 + 6CO(g)$	(R1)	2454.38–1.089T (K)	Above ~2000
$3Al_2O_3 + 6C \rightarrow Al_4CO_4 + Al_2CO + 4CO(g)$	(R2)	1582.1–0.728T (K)	Above 1920
$2Al_2O_3 + 3C = Al_4CO_4 + 2CO(g)$	(R3)	810–0.377T (K)	Above 1900

Therefore, Al_2O_3 powder can also be dispersed in water at pH 12. In other words, both purified MWCNTs and Al_2O_3 powder can be dispersed and mixed in a common medium, water at pH 12. However, the density of the CNTs, 1–2 g/cm^3, is much less than the density of Al_2O_3, ~4 g/cm^3. As a result, MWCNTs would likely segregate from Al_2O_3 powder during drying of CNT–Al_2O_3 slurries due to differential sedimentation rates driven by the difference in density. This could explain the CNT agglomerates that have been observed in some densified CNT–Al_2O_3 composites.[21] To minimize segregation of the low density MWCNTs from the heavier Al_2O_3 powder, a freeze drying technique was used in the present study. In this process, the aqueous slurry was rapidly frozen so that the CNTs and Al_2O_3 particles remained uniformly mixed through the entire drying process. Consequently, the homogeneity of the MWCNT–Al_2O_3 slurry was maintained in the dried CNT–Al_2O_3 composite powder.

3.3. Densification

Reactions between Al_2O_3 and CNTs that produce gaseous species may inhibit densification of CNT–Al_2O_3 compacts and damage the CNTs. If damage occurs, then the desired composite properties will not be achieved. Thus, a basic requirement for fabrication of CNT–Al_2O_3 composites is avoidance or minimization of reactions. Table 1 summarizes the results of thermodynamic calculations for some possible reactions in the Al_2O_3–C system. The results reveal that under standard state conditions, reactions between Al_2O_3 and C become favorable above ~1900 °C. The equilibrium constants for Reactions (R2) and (R3) drop to ~10^{-8} by 1550 °C, indicating that it is likely that Al_2O_3 and CNTs can be sintered with little or no reaction at the typical temperatures used for pressureless sintering of Al_2O_3 ceramics (e.g., ~1550 °C). However, sintering in conditions that deviate significantly from standard state may make the reactions favorable at lower temperatures. For example, sintering in the reduced pressure of a mild vacuum will reduce the temperatures at which the reactions become favorable by reducing the activity of the gaseous species in the reaction products.

To minimize possible reactions, different sintering temperatures and hold times were investigated so that full density could be reached at the lowest possible combination of temperature and time. Other researchers have commonly employed hot-pressing or SPS to fabricate CNT–Al_2O_3 composites because these techniques often reduce the temperature or time necessary to achieve full density. Based on the thermodynamic calculations, pressureless sintering should be possible without significant damage to the CNTs, if sintering temperatures around 1550 °C can be used. So, it should be possible to sinter CNT–Al_2O_3 composites without damaging the CNTs as long as densification is not inhibited by other factors.

As a baseline, nominally pure Al_2O_3 pellets were densified by heating at 5 or 10 °C/min to temperatures of 1450, 1475, 1500 and 1550 °C using a hold time of 2 h in a flowing argon atmosphere. The results indicated that Al_2O_3 reached full density at 1500 °C, which is below the temperatures required for Reaction (R2) or (R3) to proceed under standard state conditions. Based on these results, the sintering parameters selected for CNT–Al_2O_3 densification were a heating rate of 10 °C/min, for a hold time of 2 h at 1500 °C, and a flowing argon atmosphere. The densification results for the Al_2O_3 pellets and Al_2O_3 containing 1, 3 and 5 vol.% CNTs are summarized in Table 2.

Two main points can be noted from the results in Table 2. First, CNT–Al_2O_3 composites were sintered to high density at 1500 °C in flowing argon. For example, Al_2O_3 containing 1 vol.% CNTs was sintered to near full density by heating to 1500 °C for 1.5 or 2 h. Likewise, composites containing 3 and 5 vol.% CNTs were sintered to ~96 and ~92% density, respectively. Similar behavior was observed in spark plasma sintered CNT–Al_2O_3 materials.[26,28] Second, the weight loss, which is caused by reactions between Al_2O_3 and the CNTs, increased as the sintering temperature, time, and CNT content increased. For instance, the mass loss for Al_2O_3 containing 1, 3 and 5 vol.% CNTs sintered at 1500 °C for 2 h are 0.04%, 0.12% and 1.22%, respectively. According to the reactions listed in Table 1, each gram of weight loss from sintered Al_2O_3–CNT composites is equivalent to a carbon loss of ~0.43 g (0.20 cm^3) in the form of carbon monoxide (CO). The remaining weight loss was due to oxygen loss from the system. The weight losses are equivalent to CNT volume losses of 0.032% for the composite containing 1 vol.% CNTs, 0.1% for 3 vol.% CNTs and 1% for 5 vol.% CNTs. The mass loss for CNT–Al_2O_3 containing 5 vol.% CNTs increased from 1.22% after sintering at 1500 °C for 2 h to 6.95% after sintering at 1600 °C for 2 h. Along with the increase in mass loss, the relative density decreased from ~92% after sintering at 1500 °C for 2 h to ~76% after sintering at 1600 °C for 2 h. The mass losses were attributed to the negative effects of the reactions, which depleted the solid and produced gaseous products.

In addition to density and mass loss, the CNT content affected the distribution of CNTs in the composites. Small volume fraction additions resulted in individual CNTs being located on grain boundaries of the matrix phase. At higher volume fractions the CNT content was over the percolation threshold and, consequently, clusters formed. Rul et al.[4] and Hirota et al.[36] investigated the percolation threshold in this system. Based on electrical conductivity measurements, the groups reported percolation limits of 0.64 and 1.5 vol.%, respectively. The differ-

Table 2
Summary of densification results for pure Al_2O_3 and Al_2O_3 containing 1, 3 and 5 vol.% CNTs.

	Material							
	Pure Al_2O_3		Al_2O_3–1% CNT		Al_2O_3–3% CNT		Al_2O_3–5% CNT	
	ΔW%	ρ (%)	ΔW%	ρ (%)	ΔW%	ρ (%)	ΔW%	ρ (%)
Sintering conditions								
1600 °C/2 h	–	–	−0.74	97.2	−3.55	91.6	−6.95	76.4
1500 °C/2 h	0	99.8	−0.04	>99	−0.12	96.5	−1.22	91.7
1500 °C/1.5 h	–	–	~0	>99	−0.1	96.3	−0.75	92.2

Table 3
Electrical resistivity of sintered Al_2O_3 and CNT–Al_2O_3 composites.

	Material			
	Pure Al_2O_3	1 vol.% CNT	3 vol.% CNT	5 vol.% CNT
Resistivity (Ω cm)	$>10^{15}$	4.6×10^{13}	1.2×10^{4}	2.1×10^{12}

ence in percolation threshold was likely due to its dependence of the aspect ratio of the CNTs and the particle size of the ceramic. Table 3 summarizes the electrical resistivity for pure Al_2O_3, and composites containing 1, 3 and 5 vol.% CNTs prepared as part of the present study. In general, the electrical resistivity decreased as CNT content increased. Pure Al_2O_3 had a resistivity of $>10^{15}$ Ω cm, while resistivity decreased to $\sim10^{13}$ Ω cm for 1 vol.% CNTs. The addition of 3 vol.% CNTs resulted in a sharp drop in resistivity to $\sim10^{4}$ Ω cm, indicating that the conductive CNTs likely formed a spanning cluster in this material. In fact, the clusters can be observed in its microstructure photograph shown in the next section. However, the composite with 5 vol.% CNTs had a higher electrical resistance ($\sim10^{12}$ Ω cm) than the composite containing 3 vol.% CNTs, indicating that the CNTs did not form a continuous spanning cluster in this material. Considering 20 vol.% loss of the initial 5 vol.% CNTs for the composite sintered at 1500 °C, the higher electrical resistivity of this material can be attributed to the greater loss of CNTs during sintering of the material containing 5 vol.% CNTs. The combination of higher weight loss and less linear shrinkage during sintering resulted in poor contact between CNT clusters in the 5 vol.% CNT composite. Based on the densification, mass loss, and electrical resistivity measurements, the CNT content should be kept to less than 3 vol.% for composites prepared by pressureless sintering to achieve high density with minimal loss of CNTs due to reaction.

3.4. Microstructure

Fig. 3 compares the polished surfaces of nominally pure Al_2O_3 and a composite containing 1 vol.% CNTs that were sintered at 1500 °C for 2 h. As seen from the images, the average grain size of Al_2O_3 in the 1 vol.% CNT composite was ~1 μm, which was smaller than the grain size of 2–3 μm found in nominally pure Al_2O_3 sintered under the same conditions. The reduction in grain size can be attributed to grain pinning by the CNTs.[10,37] Fig. 4 compares the fracture surfaces of nominally pure Al_2O_3 and composites containing 1, 3 and 5 vol.% CNTs sintered at 1500 °C for 2 h. As seen from the images, the CNTs were intact after densification. Further, the number of CNTs observed on the fracture surfaces increased as the volume percent of CNTs added to the batch increased. These results indicated that the sintering conditions did not lead to significant CNT loss for 1 and 3 vol.% CNT additions as discussed in the last section. The CNTs appeared to be distributed homogeneously in the Al_2O_3 matrix in all three CNT–Al_2O_3 composites. Microstruc-

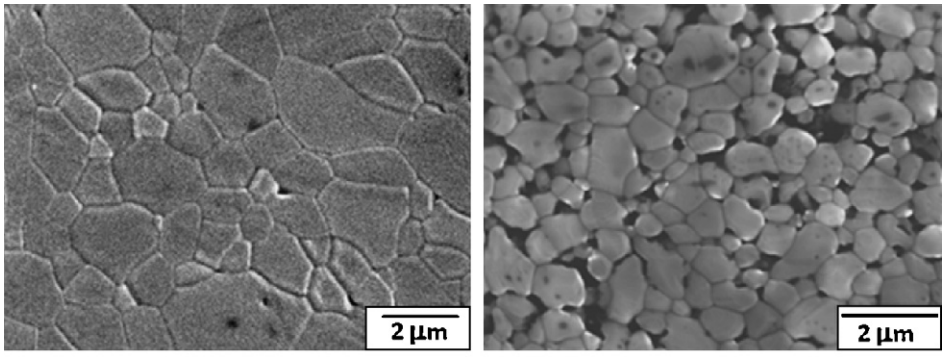

(a) nominally pure Al_2O_3 (b) 1 vol% CNT-Al_2O_3

Fig. 3. Microstructures of nominally pure Al_2O_3 and composites containing 1 vol.% CNTs sintered at 1500 °C for 2 h. (a) Nominally pure Al_2O_3; (b) 1 vol.% CNT–Al_2O_3.

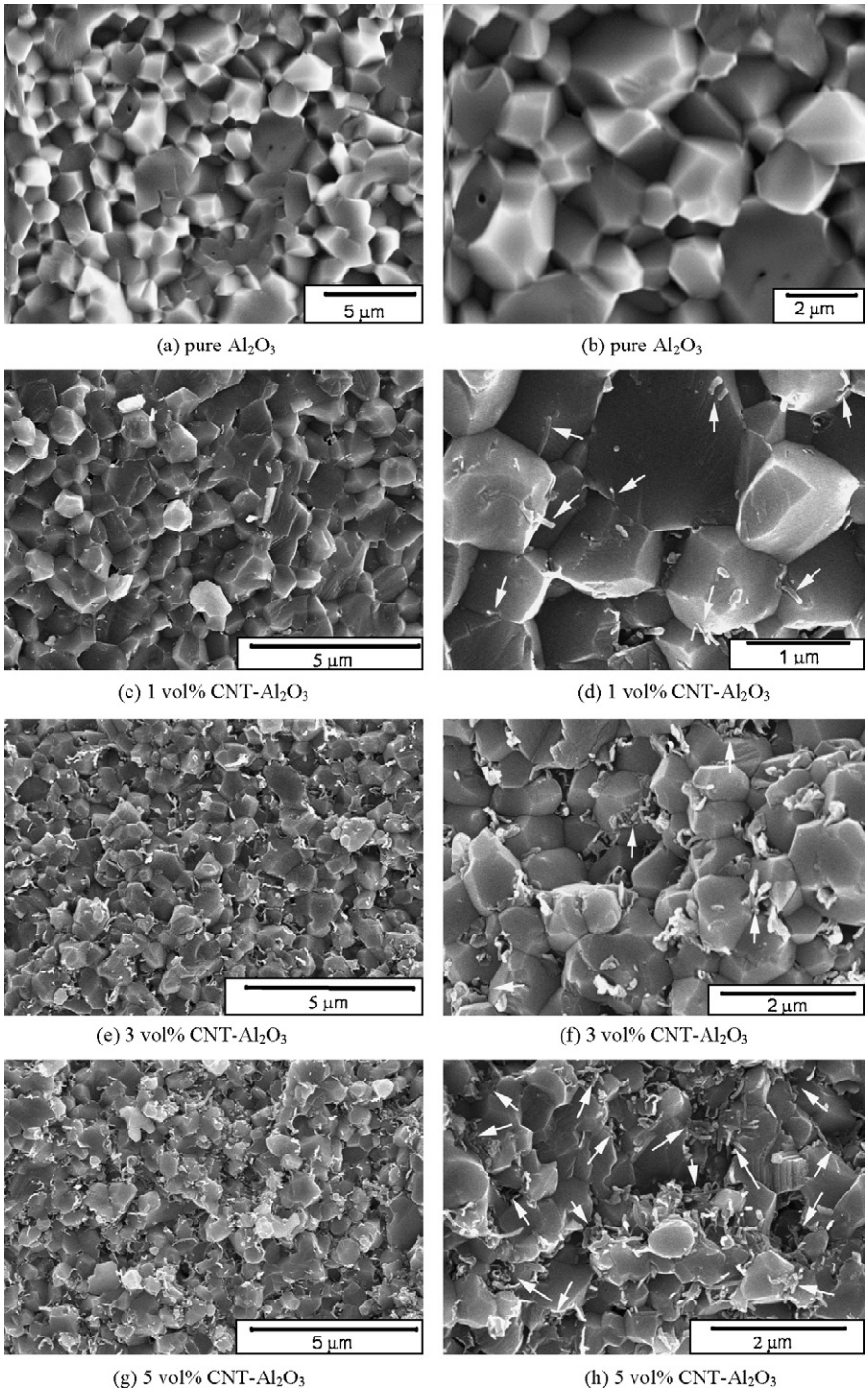

Fig. 4. Microstructures of nominally pure Al_2O_3 and composites containing 1, 3, and 5 vol.% CNTs sintered at 1500 °C for 2 h. Note that the magnifications vary among the images. Arrows in images (c) and (d) indicate individual CNTs, while arrows in images (f), and (h) indicate CNT clusters. (a and b) Pure Al_2O_3; (c and d) 1 vol.% CNT–Al_2O_3; (e and f) 3 vol.% CNT–Al_2O_3; (g and h) 5 vol.% CNT–Al_2O_3.

tural analysis indicated that the combination of the purification, dispersion, and freeze drying processes successfully overcame problems with CNT segregation as has been reported in the technical literature. However, even though the CNTs were uniformly dispersed, some clusters were still observed in the composites containing 3 and 5 vol.% CNTs because the CNT content had exceeded the percolation threshold in these compositions. The clusters are marked by arrows in the images (Fig. 4(f) and (h)).

3.5. Mechanical properties

The elastic modulus, hardness, flexure strength and fracture toughness of Al_2O_3 and composites containing 1, 3 and 5 vol.% CNTs are summarized in Table 4. The elastic modulus of CNT–Al_2O_3 composites decreased as CNT content increased. This can be explained using the theory of short fiber reinforced composites. Compared to continuous fiber reinforced

Table 4
Summary of mechanical properties of Al_2O_3 and CNT–Al_2O_3 composites.

Properties	Al_2O_3	Al_2O_3–1% CNT	Al_2O_3–3% CNT	Al_2O_3–5% CNT
Relative density (%)	99.8	>99	96.5	91.7
Young's modulus (GPa)	377 ± 37	428 ± 14	241 ± 20	233 ± 17
Hardness (GPa)	23.2	22.3	17.9	12.6
Flexure strength (MPa)	403 ± 79	543 ± 37	364 ± 31	286 ± 23
Toughness (MPa $m^{1/2}$)	3.3 ± 0.5	4.1 ± 0.6	3.5 ± 0.4	3.6 ±0.5

composites, the Young's modulus of the composites reinforced by aligned short fibers can be expressed using Eq. (1)[37]:

$$E_{11} = \eta_l E_f \upsilon_f + E_m(1 - \upsilon_f) \quad (1)$$

where E_{11} is the Young's modulus along the longitudinal fiber direction, E_m is the Young's modulus of the matrix, and υ_f is the volume fraction of the continuous fiber. Because the reinforcing efficiency of short fibers is less than continuous fibers, a length efficiency parameter, η_l, is included in Eq. (1) for fibers less than some critical length (l_c). For non-aligned systems, the reinforcing efficiency of the short fiber is reduced further. An additional orientation efficiency factor, η_o, can be introduced into Eq. (1) to produce Eq. (2):

$$E_{11} = \eta_l \eta_o E_f u_f + E_m(1 - \upsilon_f) \quad (2)$$

where η_o is the orientation efficiency factor, which has been taken as 0.2 for a random three-dimensional dispersion of short fibers.[37]

Considering that CNTs have an ultra-high Young's modulus and a high aspect ratio (length of 0.5–2 μm and diameter of 30–40 nm), the average CNT length in the present study was greater than the critical length, l_c.[38] Therefore, Eq. (2) can be used to estimate Young's modulus of the CNT-reinforced Al_2O_3 composites. The first group of factors in Eq. (2) ($\eta_l\eta_o$) is zero when no CNTs are added, i.e. the Young's modulus of nominally pure sintered Al_2O_3 should be equal to the intrinsic modulus of Al_2O_3. The sintered CNT–Al_2O_3 composite containing 1 vol.% CNTs was >99% theoretical density. Therefore, the second term of Eq. (2) should be about 1% less than the Young's modulus of nominally pure Al_2O_3. However, the first item is not zero and the effective Young's modulus of the composite should be higher than nominally pure Al_2O_3, if the Young's modulus of the CNTs in the lengthwise direction (~1 TPa) is considered. When the CNT content is increased the sintered densities drop to 96 and 91% of the theoretical density for 3 and 5 vol.% CNTs, respectively. The decrease in density will cause a significant decrease in the value of the second term of Eq. (2), which is larger than the increase in Young's modulus predicted by the first term. As a result, the addition of 3 or 5 vol.% CNTs results in a lower Young's modulus than nominally pure Al_2O_3 as shown in Table 4. The hardness of the composites follows the same trend as Young's modulus, presumably for the same reasons.

The composite containing 1 vol.% CNTs had a higher flexure strength (~540 MPa) and fracture toughness (4.1 MPa $m^{1/2}$) than nominally pure Al_2O_3 (strength ~400 MPa and toughness ~3.3 MPa $m^{1/2}$). From the SEM micrographs shown in Fig. 3, the average grain size of nominally pure Al_2O_3 was 2–3 μm while the average Al_2O_3 grain size for the composite containing 1 vol.% CNTs was ~1 μm. Therefore, the higher strength appears to be due to the smaller grain size of the composite. The smaller grain size may have resulted from the pinning effect of the CNTs that were homogeneously distributed on Al_2O_3 grain boundaries.[10] At CNT contents of 3 and 5 vol.%, the strength dropped to less than 250 MPa. The lower strengths of these materials are likely due to the fact that the CNT contents were over the percolation threshold for CNTs in the Al_2O_3 matrix. Even though the percolation threshold is greatly dependent on the aspect ratio of CNTs, and the Al_2O_3 particle size, it can still be concluded that 3 vol.% CNTs was over the percolation threshold in the present system as the electric resistance of the sintered composites dropped from 10^{13} Ω cm for 1 vol.% to 10^4 Ω cm for 3 vol.% CNTs. In addition, some clusters were present at the higher CNT contents as shown in the microstructures of the 3 and 5 vol.% CNTs samples. In this case, bundles of CNTs likely acted as flaws[28] and resulted in the lower observed fracture strength.[26,38]

As shown in Table 4, the composite containing 1 vol.% CNTs had the highest fracture toughness, 4.1 MPa $m^{1/2}$, of all of the materials tested. Compared to nominally pure Al_2O_3, the 1 vol.% CNT composite had a higher fracture strength and smaller grain size (Fig. 3(b)), which resulted in a smaller possible size for strength-limiting flaws. Some fiber pullout was observed in the 1 vol.% CNT composite as indicated by arrows in Fig. 4(d). In addition, crack deflection and crack bridging effects may also contribute to the higher fracture toughness of this material. The combination of all of the factors resulted in the highest fracture toughness for the 1 vol.% CNT composite. However, fracture toughness of Al_2O_3–CNT composites decreased with increasing CNT content above 1 vol.%, even though the toughness values were still higher than nominally pure Al_2O_3. The decrease in fracture toughness may have resulted from poor bonding at the interface between bundles of CNTs and Al_2O_3 grains.

4. Conclusions

Alumina matrix composites containing 1, 3 and 5 vol.% CNTs were successfully densified using pressureless sintering for the first time. Commercial MWCNTs were purified, dispersed, and homogeneously mixed with Al_2O_3 powder in water at pH 12. The slurry of CNTs and Al_2O_3 was freeze dried to maintain its homogeneity. Pellets of the Al_2O_3–CNT composite powder were sintered to high density without externally applied pressure. The following conclusions were drawn from the study:

(1) The combination of CNT purification and freeze drying of the Al_2O_3–CNT suspension resulted in a uniform distribution of CNTs in an Al_2O_3 matrix.
(2) Al_2O_3–CNT composites were densified using pressureless sintering when the CNT content was kept below 3 vol.%. Reactions between Al_2O_3 and the CNTs, which could lead to CNT loss, were limited by keeping the sintering temperature to 1550 °C or below.
(3) The composite containing 1 vol.% CNTs had a higher flexure strength (~540 MPa) than nominally pure Al_2O_3 (~400 MPa). The increase in strength was attributed to the inhibition of grain growth in the Al_2O_3 composite due to the pinning effect of the CNTs at the grain boundaries. Flexure strengths of composites with higher CNT contents were lower (230–240 MPa) due to the presence of porosity and clusters of CNTs in the composites.
(4) Compared to nominally pure Al_2O_3, the fracture toughness values for all Al_2O_3–CNT composites were improved due to the CNT content.

References

1. Iijima S. Helical microtubules of graphitic carbon. *Nature (London)* 1991;**354**:56–8.
2. Harries PJF. Carbon nanotube composites. *Int Mater Rev* 2004;**49**(1):31–42.
3. Yu MF, Lourie O, Dyer MJ, Molor K, Kelly TF, Ruoff RS. Strength and breaking mechanism of multiwalled carbon nanotubes under tensile loads. *Science* 2000;**287**:637–40.
4. Rul S, Lefevre-Schlick F, Capra E, Laurent Ch, Peigney A. Percolation of single-walled carbon nanotubes in ceramic matrix nanocomposites. *Acta Mater* 2004;**52**:1061–7.
5. Qian D, Dickey EC. Load transfer and deformation mechanism in carbon nanotube–polystyrene composite. *Appl Phys Lett* 2000;**76**:2868–79.
6. Kuzumaki T, Miyazawa K, Ichinose H, Ito K. Processing of carbon nanotube reinforced aluminum composite. *J Mater Res* 1998;**13**:2445–9.
7. Wanfer HD, Lourie O, Feldman Y, Tenne R. Stress-induced fragmentation of multiwall carbon nanotubes in a polymer matrix. *Appl Phys Lett* 1998;**72**(2):188–90.
8. Lourie O, Wanfer HD. Evidence of stress transfer and formation of fracture clusters in carbon nanotube-based composites. *Compos Sci Technol* 1999;**59**(6):975–7.
9. Schadle LS, Giannaris SC, Ajayan PM. Load transfer in carbon nanotube epoxy composites. *Appl Phys Lett* 1998;**73**(26):3842–4.
10. Flahaut E, Peighey A, Laurent Ch, Marliere Ch, Chastel F, Rousset A. Carbon nanotube–metal–oxide nanocomposites: microstructure, electrical conductivity and mechanical properties. *Acta Mater* 2000;**48**:3803–12.
11. Ajayan PM, Stephan O, Colliex C, Trauth D. Aligned carbon nanotube arrays formed by cutting a polymer resin–nanotube composite. *Science* 1994;**265**:1212.
12. Shadler LS, Giannaris SC, Ajayan PM. Load transfer in carbon nanotube epoxy composite. *Appl Phys Lett* 1998;**73**:3842.
13. Bower C, Rosen R, Jin L, Han J, Zhou O. Deformation of carbon nanotubes in nanotube–polymer composites. *Appl Phys Lett* 1999;**74**:3317.
14. Wanger HD, Lourie O, Feldman Y, Tenne R. Stress-induced fragmentation of multiwall carbon nanotubes in a polymer matrix. *Appl Phys Lett* 1998;**72**:188.
15. Lourie O, Wanger HD. Evidence of stress transfer and formation of fracture clusters in carbon nanotube-based composites. *Compos Sci Technol* 1999;**59**:975.
16. Xu CL, Wei BQ, Ma J, Liang RZ, Ma XK, Wu DH. Fabrication of aluminum–carbon nanotube composites and their electrical properties. *Carbon* 1999;**37**:855–8.
17. Siegel RW, Chang SK, Ash B'J, Stone J, Ajayan PM, Doremus RW, et al. Mechanical behavior of polymer and ceramic matrix nanocomposites. *Scripta Mater* 2001;**44**:2061–4.
18. Kumari L, Zhang T, Du GH, Li WZ, Wang QW, Datye A, et al. Thermal properties of CNT–Al_2O_3 nanocomposites. *Compos Sci Technol* 2008;**68**:2178–83.
19. Wei Z, Fan Z, Luo G, Wei F, Zhao D, Fan J. The effect of carbon nanotubes microstructures on reinforcing properties of SWNTs/alumina composite. *Mater Res Bull* 2008;**43**:2806–9.
20. Sun J, Gao L, Jin X. Reinforcement of alumina matrix with multi-walled carbon nanotubes. *Ceram Int* 2005;**31**:893–6.
21. Fan J, Zhao DQ, Wu MS, Xu Z, Song J. Preparation and microstructure of multi-wall carbon nanotube-toughned Al_2O_3 composite. *J Am Ceram Soc* 2006;**89**(2):750–3.
22. Xia Z, Curtin WA, Sheldon BW. Fracture toughness of high ordered carbon nanotube/alumina nanocomposites. *Trans ASME* 2004;**126**:238–44.
23. Huang Q, Gao L. Manufacture and electrical properties of multiwalled carbon nanotube/$BaTiO_3$ nanocomposites. *J Mater Chem* 2004;**14**:2536–41.
24. Peigney A, Laurent CH, Flahaut E, Rousset A. Carbon nanotubes in novel ceramic matrix nanocomposites. *Ceram Int* 2006;**26**:677–83.
25. Zhan GD, Kuntz J, Wan J, Mukherjee AK. Single-wall carbon nanotubes as attractive toughening agents in alumina-based nanocomposites. *Nat Mater* 2003;**2**:38–42.
26. Woodman RH, Klotz BR, Dowding RJ. Evaluation of a dry ball-milling technique as a method for mixing boron carbide and carbon nanotube powder. *Ceram Int* 2005;**31**:765–8.
27. Laurent Ch, Peigney A, Dumortier O, Rousset A. Cabon nanotubes–Fe–alumina nanocomposites. Part II. Microstructure and mechanical properties of hot-pressed composites. *J Eur Ceram Soc* 1998;**18**:2005–13.
28. Zhang T, Kumari L, Du GH, Li WZ, Wang QW, Balani K, et al. Mechanical properties of carbon nanotube–alumina nanocomposites synthesized by chemical vapor deposition and spark plasma sintering. *Composites, Part A* 2009;**40**:86–93.
29. Kong J, Casell AM, Dai H. Chemical vapor deposition of methane for single-walled carbon nanotubes. *Chem Phys Lett* 1998;**292**:567–74.
30. Park TJ, Banerjee S, Hemjaj-Benny T, Wong S. Purification strategies and purity visualization techniques for single-walled carbon nanotubes. *J Mater Chem* 2006;**16**:141–54.
31. Okada K, Sakuma T. The role of Zener pinning effect on the grain-growth in Al_2O_3–ZrO_2. *J Ceram Soc Jpn* 1992;**100**:382–6.
32. Rahaman MN. *Ceramic processing and sintering*. New York: Marcel Dekker; 1995 [chapter 11].
33. CNT resource data from www.nanoamor.com.
34. Poyato R, Vasiliev AL, Padture NP, Tanaka H, Nishimura T. Aqueous colloidal processing of single-wall carbon nanotubes and their composites with ceramics. *Nanotechnology* 2006;**17**:1770–7.
35. Chantikul P, Anstis GR, Lawn GR, Marshall DB. A critical evaluation of indentation techniques for measuring fracture toughness. II. Strength method. *J Am Ceram Soc* 1981;**64**:539–43.
36. Hirota K, Takaura Y, Kato M, Miyamoto Y. Fabrication of carbon nanofiber (CNT)-dispersed Al_2O_3 composites by pulsed electric-current pressure sintering and their mechanical and electrical properties. *J Mater Sci* 2007;**42**:4792–800.
37. Matthews FL, Rawlings RD. *Composite materials: engineering and science*. CRS Press; 1999.
38. Ning JW, Zhang JJ, Pan YB, Guo JK. Fabrication and mechanical properties of SiO_2 matrix composites reinforced by carbon nanotube. *Mater Sci Eng A* 2003;**357**:392–6.